ENRI Int. Workshop on ATM/CNS. Tokyo, Japan (EIWAC2017)

[EN-A-025] Integrated Bi-level Arrival and Departure Time Assignment for Optimal Trajectories

+ B. Grüter * J. Diepolder * T. Akman * F. Holzapfel *

* Institute of Flight System Dynamics,
Technical University of Munich
Munich, Germany
[benedikt.grueter | johannes.diepolder | tugba.akman | florian.holzapfel]@tum.de

Abstract: In this paper, we present a bi-level algorithm, which provides an optimal time assignment for arriving and departing aircraft with respect to the overall fuel consumption of all arriving and the delay of departing aircraft. The optimal arrival time assignment is performed by the upper level of the bi-level structure, avoiding the solution of a costly combinatorial problem. The upper level optimization is subject to separation constraints, which ensure operational safety on the one hand, and a feasible solution in the lower levels on the other hand. The lower level optimal control problems define the optimal trajectories of each individual aircraft, respecting the arrival times assigned by the upper level problems as well as a safe distance separation with respect to all other aircraft. The objective functions of both levels within the bi-level optimization are the minimization of consumed fuel, the individual fuel consumption in the lower level problem, and the combined fuel of all aircraft in the upper level. Hence, the bi-level algorithm constitutes a primal decomposition of a combined, multi-aircraft optimal control problem.

Keywords: Air Traffic Management, Arrival and Departure Management, Arrival Time Assignment, Primal Decomposition

1 INTRODUCTION

Air traffic has undergone a steady growth in the last decades and is expected to continue growing at a constant rate [1]. This will inevitably lead to a lack of capacity, especially at bottlenecks of the system, such as large aerodromes. The resulting challenges can only be met by extending the current infrastructure or introducing novel procedures that increase its performance. Within the process, which is driven by national and international programs, such as SESAR, NextGen, and CARATS, technologies are already developing with a high potential of improving performance, such as i4D trajectories, E-AMAN, and SWIM. These technologies will in turn enable the exploitation of highly advanced methods, especially in the field of optimization.

The technical development in aviation and computational power also enable advanced research in the field of the numerical optimization of arrival management. The studies [2, 3] combine several aircraft into a single, large scale optimal control problem, which is solved by applying direct collocation methods. [4] proposes a simultaneous optimization of trajectory and sequence by calculating a criterion function using indirect optimal control methods and varying the final time. A genetic algorithm is employed in [5] to optimize sequences and trajectories in a bi-level approach. Furthermore, a gradient-based method for an optimal arrival time assignment is presented in [6], which includes a homotopy approach to facilitate the solution process by gently removing a relaxation in the constraints.

In this work, a bi-level approach is presented that can treat the problem in a single run without the need to employ a homotopy approach. Furthermore, the capacity reduction due to departing aircraft can be considered in this approach. The bi-level structure is displayed in Fig. 1, which shows the flow of information during the solution process between the upper level to calculate the optimal arrival times and the lower level problem defining the optimal trajectories. The novel upper level problem structure is presented in section 2, followed by a short introduction of the models in section 3, and the optimal control problems in section 4. Finally, a case study is presented in section 5 before concluding the paper in section 6.

2 ARRIVAL TIME ASSIGNMENT

The upper level problem is formulated to define the optimal arrival times of all aircraft, respecting the constraints on time and distance separations at the final approach fix (FAF). Hereby, the objective function to be maximized is the cumulated final mass $m_{1,i}$ of all aircraft

$$i = 1 \dots n_{ac} \tag{1}$$

at the FAF, which is equivalent to minimizing the cumulated fuel consumption of all n_{ac} arriving aircraft.

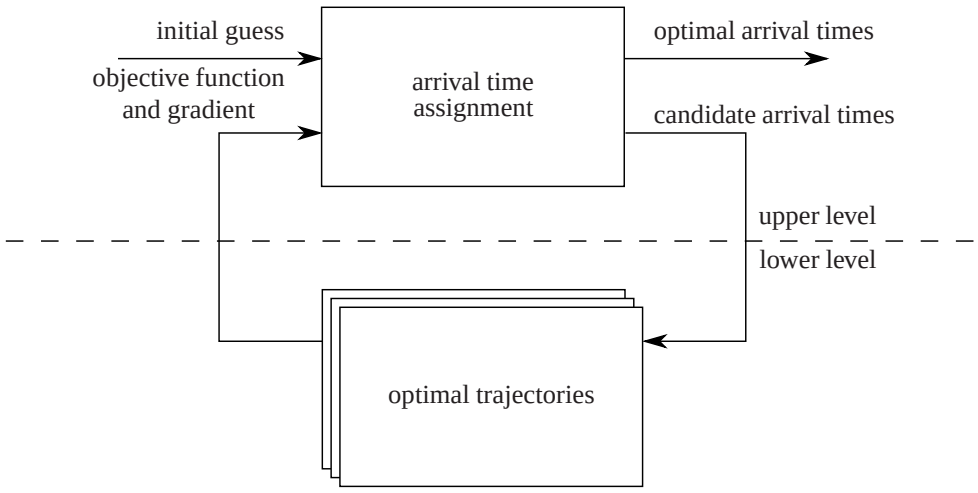

Figure 1: Bi-level structure resulting from the primal decomposition of the multi aircraft approach problem.

Table 1: Separation based on the *wake turbulence categories* L(ight), M(edium), H(eavy) and S(uper Heavy) of preceding (row) and following aircraft (column). [7]

(a) Time separation in *min*

	L	M	H	S
L	0	0	0	0
M	3	2	0	0
H	3	2	0	0
S	3	3	2	0

(b) Horizontal distance separation in *nm*

	L	M	H	S
L	3	3	3	3
M	5	3	3	3
H	6	5	4	4
S	8	5	4	4

Hence, the upper level optimization problem yields:

$$\hat{\mathbf{t}}^* = \arg\min_{\hat{\mathbf{t}}} \sum_{i=1}^{n_{ac}} -m^*_{1,i}(\hat{t}_i) + \theta \cdot \sum_{j=1}^{n_{ac,dep}} \left(\hat{t}_j - t_{j,des}\right)^2, \quad (2)$$

where $\hat{t}_i$ denotes the arrival time of aircraft i at the FAF. Additionally, equation (2) shows a second term penalizing the delay of the $n_{ac,dep}$ departing aircraft. The penalty is subject to the weighing factor θ.

This problem is constrained by a pairwise separation between all aircraft arriving at the FAF. On the one hand, the time separations according to ICAO Doc. 4444 [7], which is listed in Tab. 1a, have to be respected. However, the sequence of arriving aircraft is not known a priori, hence only one of the two constraints

$$\hat{t}_i - \hat{t}_j - \Delta t_{ji} \leq 0, \quad (3)$$
$$\hat{t}_j - \hat{t}_i - \Delta t_{ij} \leq 0, \quad (4)$$

is valid, where Δt_{ji} denotes the minimum time separation between the leading aircraft j and the following aircraft i and vice versa. Because of the dependency of this minimum time separation on the wake turbulence category of both aircraft, the minimum time separation is generally not symmetric:

$$\Delta t_{ji} \neq \Delta t_{ij}. \quad (5)$$

This problem is solved by combining the time separation constraints for each pair of aircraft to a single quadratic constraint introduced in [6], which is depicted in Fig. 2:

$$c_{\hat{t},ij} = \left(\hat{t}_i - \hat{t}_j - \frac{\Delta t_{ji} - \Delta t_{ij}}{2}\right)^2 - \left(\frac{\Delta t_{ji} + \Delta t_{ij}}{2}\right)^2 \geq 0, \, i \neq j. \quad (6)$$

This constraint formulation simultaneously ensures a safe time separation for the considered pair of aircraft, regardless of the order of reaching the FAF. Hereby, the difference of arrival times

$$\hat{t}_i - \hat{t}_j \quad (7)$$

takes positive values, if aircraft j arrives before aircraft i. In this case, aircraft j is the leading aircraft and the time separation Δt_{ji} has to be respected, which is zero in the example of heavy aircraft following the medium. In the opposite case, i.e. for the medium aircraft following a heavy, the difference takes negative

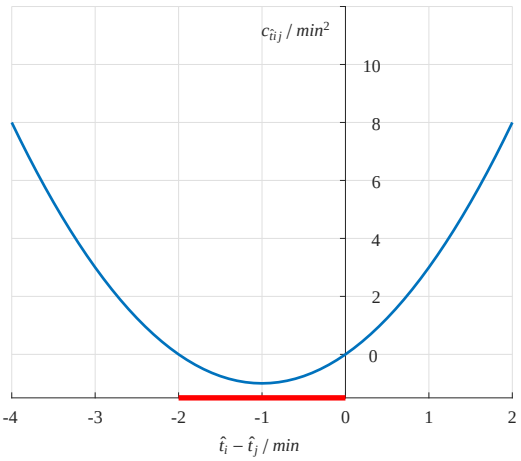

Figure 2: Combined time separation constraint function between aircraft i (H) and j (M).

values and the respective required time separation is 2 min, according to Tab. 1a.

In contrary to the formulation presented in [6], the distance separation at the FAF is also considered in the upper level problem extending the list of constraints. This approach is chosen to mitigate the drawback that the upper level problem does not contain any information about the distance separation in the lower level problem. Therefore, the solution of the upper level problem may yield a pair of equal arrival times for any case, whenever Tab. 1a yields no time separation. However, this contradicts with the non-zero distance separation path constraint comprised in the lower level optimal control problems, which has to be respected along the entire trajectory and thus also at the FAF.

The inclusion of the distance separation at the FAF within the upper level optimization ensures the feasibility of the lower level optimal control problems. Similarly to the time separation constraint, the required distance separation depends on the order of arriving aircraft. Consequently, equation (6) can either be applied analogously or reused for the distance separation at the FAF by adjusting the required time separation Δt_{ji}. The time difference between two adjacent aircraft required to ensure a safe distance separation can be calculated by deriving the distance $d_{i,FAF}$ of the following aircraft i to the FAF from its trajectory, where the condition for the required time separation $\Delta t_{ji,d}$, which is implicitly defined by the required distance separation $d_{ji,WTC}$, holds:

$$d_{i,FAF}\left(\hat{t}_i - \Delta t_{ji,d}\right) = d_{ji,WTC}. \tag{8}$$

The required distance separation of each combination of aircraft of different wake turbulence categories are tabulated in Tab. 1b. The overall required time separation follows as the maximum of the time separation given directly by the ICAO (Tab. 1a) and the time separation implied by the distance separation (Tab. 1b):

$$\Delta t_{ji} = \max\left\{\Delta t_{ji,WTC}, \Delta t_{ji,d}\right\}. \tag{9}$$

The constraint given by equation (9) is introduced into the optimization problem by including the required time separation Δt_{ji} for each combination of leading aircraft j and following aircraft i as additional optimization variables into the upper level problem problem. Furthermore, two constraints are introduced for each of the additional variables:

$$c_{\Delta t_{ji,WTC}} = \Delta t_{ji} - \Delta t_{ji,WTC} \geq 0, \tag{10}$$
$$c_{\Delta t_{ji,d}} = \Delta t_{ji} - \Delta t_{ji,d} \geq 0. \tag{11}$$

For a runway operating at full capacity, the problem is well defined and has a unique solution, where the required time separation takes the value of the maximum of the two values respecting the time and distance separation defined by the ICAO. If the optimal solution contains inefficiencies in a way, that the duration between two arriving aircraft is larger than the respective minimum time separation, an additional term has to be added to the objective function, e.g. by adding the sum of the required time separations, which are positive by definition:

$$\sum_i \sum_j \Delta t_{ji}, \quad i \neq j. \tag{12}$$

After introducing a continuous formulation of the sequencing problem, the choice of approaches for the solution can be extended by gradient-based methods. In this work, the SQP algorithm of the *fmincon* solver included in Matlab is utilized. This solver requires the gradient of objective and constraint functions with respect to all optimization variables. The objective function J of the upper level problem contains the final mass of all aircraft, which is determined by the lower level optimal control problems. Hence, for a simple problem containing only two aircraft 1 and 2, the optimization vector is

$$\mathbf{z} = (\hat{t}_1, \hat{t}_2, \Delta t_{12}, \Delta t_{21})^T \tag{13}$$

and the gradient:

$$\nabla J = \begin{bmatrix} \frac{\partial m_{1,1}}{\partial \hat{t}_1} & \frac{\partial m_{2,2}}{\partial \hat{t}_2} & 0 & 0 \end{bmatrix}. \tag{14}$$

Similarly, the Hessian of the problem yields

$$\nabla^2 J = \begin{bmatrix} \frac{\partial^2 m_{1,1}}{\partial \hat{t}_1^2} & 0 & 0 & 0 \\ 0 & \frac{\partial^2 m_{2,2}}{\partial \hat{t}_2^2} & 0 & 0 \\ 0 & 0 & 0 & 0 \\ 0 & 0 & 0 & 0 \end{bmatrix}. \tag{15}$$

Furthermore, the gradient of the constraint function yields:

$$\nabla c = \begin{bmatrix} 2a & -2a & (a-b) & -(a-b) \\ 0 & 0 & 1 & 0 \\ 0 & -\frac{\partial \Delta t_{12,d}}{\partial \hat{t}_2} & 1 & 0 \\ 0 & 0 & 0 & 1 \\ -\frac{\partial \Delta t_{21,d}}{\partial \hat{t}_1} & 0 & 0 & 1 \end{bmatrix}^{\top}, \tag{16}$$

where the parameters

$$a = \left(\hat{t}_1 - \hat{t}_2 - \frac{\Delta t_{12} - \Delta t_{21}}{2} \right) \tag{17}$$

and

$$b = \frac{\Delta t_{12} + \Delta t_{21}}{2} \tag{18}$$

represent the vertex $(a, -b)$ of the parabola defined in equation (6). The Hessian of the constraint function requires the second order derivative of the variable $\Delta t_{ij,d}$, i.e. the time separation required to fulfill the distance separation at the FAF, which cannot be obtained in a straightforward way. However, the constraint can be linearized around the current point, yielding

$$\frac{\partial^2 \Delta t_{ij,d}}{\partial \hat{t}_i^2} = 0. \tag{19}$$

Alternatively, the Hessian matrix of the constraint function is estimated, e.g. by calculating BFGS updates [9].

3 MODELING

The optimal control problems for each individual aircraft respecting the arrival time fixed by the upper level problem define the optimal trajectories. To achieve realistic results with regard to the dynamic behavior of the aircraft, models for the aircraft and constraints have to be considered. In this section, the modeling of the dynamic constraints governing the system dynamics of the aircraft and the algebraic constraints ensuring a minimum distance separation are discussed.

3.1 Aircraft

The aircraft model considered within the optimal control problem has to fulfill opposing requirements: It must be sufficiently elaborate to display the flight performance properties of the real aircraft, especially with respect to the fuel consumption. However, the evaluation of the model has to show maximum efficiency to allow for short calculation times. Therefore, a point mass model of the aircraft is employed described by the seven states displayed in Tab. 2.

Table 2: States and controls for the point mass aircraft model along with their min and max values.

	Description	Min	Max
φ	geodetic latitude	$-90°$	$90°$
λ	geodetic longitude	$-180°$	$180°$
h	altitude above reference ellipsoid	$5000\ ft$	∞
V_K	kinematic speed	$V_{k,min}$	$V_{k,max}$
χ_K	flight path azimuth angle	$-180°$	$180°$
γ_K	flight path climb angle	$-\frac{\pi}{2}$	0
m	aircraft mass	ZFW_k	m_0
α_K	kinematic angle of attack	$-8°$	$12°$
μ_K	kinematic bank angle	$-30°$	$30°$
δ_T	thrust lever position	0	1

The position of the aircraft is propagated in WGS84 coordinates comprising the geodetic latitude φ, longitude λ, and the height h above the reference ellipsoid, which has a lower bound at the transition altitude of $5000\ ft$. The velocity $\vec{\mathbf{V}}_K$ of the aircraft is given in the kinematic reference frame, which is defined with respect to the north-east-down frame by the flight path climb angle γ_K and the flight path azimuth angle χ_K. Considering

- the Coriolis and centrifugal forces due to the rotation of the earth $\vec{\boldsymbol{\omega}}^{IE}$,
- the transport rate $\vec{\boldsymbol{\omega}}^{EO}$ induced by moving along the elliptical surface of the earth,
- and the centrifugal force due to the curvature of the trajectory, represented by the rotational velocity of the kinematic frame $\vec{\boldsymbol{\omega}}^{OK}$,

the differential equations for the velocity can be derived in the kinematic frame according the Newton's second law [10]:

$$\begin{aligned} & \dot{\vec{\mathbf{V}}}_K + \left(\vec{\boldsymbol{\omega}}^{OK}\right)_K \times \left(\vec{\mathbf{V}}_K\right)_K^E \\ + \; & \underbrace{\left(\vec{\boldsymbol{\omega}}^{EO}\right)_K \times \left(\vec{\mathbf{V}}_K\right)_K^E}_{\text{round earth}} \\ + \; & \underbrace{2 \cdot \left(\vec{\boldsymbol{\omega}}^{IE}\right)_K \times \left(\vec{\mathbf{V}}_K\right)_K^E - \left(\vec{\boldsymbol{\omega}}^{IE}\right)_K \times \left[\left(\vec{\boldsymbol{\omega}}^{IE}\right)_K \times \left(\vec{\mathbf{r}}^{G}\right)_K\right]}_{\text{rotating earth}} \\ = \; & \frac{1}{m} \sum \left(\vec{\mathbf{F}}\right)_K, \end{aligned} \tag{20}$$

where m denotes the mass of the aircraft. The sum of all external forces acting on the aircraft are the gravitational (G) force (denoted in the north-east-down coordinate frame O)

$$\left(\vec{\mathbf{F}}_G\right)_O = \begin{pmatrix} 0 \\ 0 \\ m \cdot g \end{pmatrix}_O, \tag{21}$$

the propulsive (P) force, which is estimated to be colinear with the kinematic velocity (denoted in the kinematic frame K)

$$\left(\vec{\mathbf{F}}_P\right)_K = \begin{pmatrix} T(\delta_T) \\ 0 \\ 0 \end{pmatrix}_K, \tag{22}$$

and the aerodynamic (A) force, consisting of the lift L and drag D (denoted in the aerodynamic frame A)

$$\left(\vec{\mathbf{F}}_A\right)_A = \begin{pmatrix} -D(\alpha_A) \\ 0 \\ -L(\alpha_A) \end{pmatrix}_A. \tag{23}$$

The propulsive and aerodynamic forces depend on the thrust lever position δ_T and the aerodynamic angle of attack α_A respectively, which are considered control variables of the aircraft model. Both forces are modeled according to the Base of Aircraft Data family 3 (BADA 3) published by EUROCONTROL [11]. The gravitational and aerodynamic forces are transformed to the kinematic reference frame using the rotation matrices $\mathbf{M}_{KO}$ and $\mathbf{M}_{KA}$, which are also used to determine the aerodynamic angle of attack α_A by coefficient comparison. Finally, the third control variable, i.e. the kinematic bank angle μ_K, is used to rotate the lift vector around the roll x-axis of the kinematic frame to provide a centripetal force. The equation of motion of the aircraft mass m

$$\dot{m} = -\dot{m}_B(\delta_T). \tag{24}$$

is modeled according to BADA 3 and thus dependent on the thrust lever position.

3.2 Safe Distance Separation

Besides the dynamic constraints introduced in the previous section, the optimal control problem is subject to algebraic path constraints, such as the minimum distance separation with respect to all other aircraft, which are modeled according to [5]. The constraints are modeled as an elliptic cylinder to respect either the vertical separation minimum $d_h = 2000\,ft$ [7] or the horizontal separation minimum d_x, which is defined by ICAO [7] and displayed in Tab. 1b. The mathematical representation of this cylinder is the maximum norm

$$d_x - \left\| \left(\sqrt{\Delta x^2 + \Delta y^2}, \frac{d_x}{d_h}\Delta h \right) \right\|_\infty \leq 0, \tag{25}$$

which may cause numerical problems due to the non-finite gradients at the sharp edges. Hence, the constraints are relaxed using the p-norm

$$-\left[\left| \sqrt{\Delta x^2 + \Delta y^2} \right|^p + \left| \frac{d_x}{d_h}\Delta h \right|^p \right]^{\frac{1}{p}} \leq -d_x, \tag{26}$$

which can be used to smoothen the sharp edges of the cylinder shape by adjusting the parameter p.

4 OPTIMAL CONTROL

The optimal control problem of each aircraft defines the optimal trajectories with respect to the individual fuel consumption under the constraint that each aircraft respects the arrival time given by the upper level optimization problem. Hence, the problem can be formulated as

$$\left[\mathbf{x}_i^*(t), \mathbf{u}_i^*(t)\right] = \underset{\mathbf{u}_i(t)}{\arg\min} - m_{1,i}. \tag{27}$$

The problem is subject to dynamic and algebraic constraints, which are introduced in the following sections.

4.1 Algebraic Constraints

The algebraic constraints for the optimal control problem can be subdivided into two different groups. Boundary conditions determine the start and end points of the state trajectory, whereas path constraints have to be fulfilled at every point in time.

4.1.1 Boundary Conditions

The initial boundary conditions

$$\psi(\mathbf{x}_0) = 0 \tag{28}$$

correspond to the flight condition and position of the aircraft when entering the terminal maneuvering area (TMA). The corresponding navigation fixes are listed in Tab. 3. Similarly, the final boundary conditions

$$\psi(\mathbf{x}_1) = 0 \tag{29}$$

are related to the final position along the trajectory, which is defined to be the FAF of runway 08L (*MAGAT*) of Munich Airport. Besides the position, the aircraft should have reached a specific velocity $V_{K,app}$ at this point. Furthermore, it should be aligned with the runway, i.e. fly at a flight path azimuth angle of

$$\chi_{K,1} = 82^\circ \tag{30}$$

, which is equal to the runway heading, and display a descent angle of

$$\gamma_{K,1} = -3^\circ \tag{31}$$

to obey the glide slope. A summary of these conditions can be found in Tab. 4.

Finally, the initial and final times are fixed within the optimal control problem. On the one hand, the initial time is different for each aircraft and represents the time of entering the TMA. On the other hand, the final time of the trajectory is dictated by the upper level algorithm and introduced as a constraint to the lower level optimal control problems:

$$c_{\hat{t}} = t_1 - \hat{t} = 0. \tag{32}$$

Table 3: Initial and final waypoints of all aircraft.

Waypoint	Latitude	Longitude
AKANU	49° 03′ 06″	10° 39′ 30″
ANORA	48° 57′ 00″	10° 32′ 54″
RIXED	48° 49′ 48″	10° 25′ 06″
ABGAS	48° 35′ 36″	10° 23′ 30″
MAGAT	48° 20′ 30″	11° 29′ 48″

Table 4: Final boundary conditions.

	State	Final Boundary
φ	latitude	48° 20′ 30″
λ	longitude	11° 29′ 48″
h	altitude	5000 ft
V_K	kinematic speed	$V_{k,app}$
χ_K	azimuth	82°
γ_K	path climb angle	−3°

4.1.2 Path Inequality Constraints

Similarly to the boundary conditions, the path inequality constraints are used to shape the optimal trajectories to display realistic results. However, the path constraints have to be fulfilled at every point of time. Among these constraints is the minimum distance separation introduced in section 3.2. Furthermore, operational constraints are added to obtain realistic trajectories, such as a limitation of the load factor in the z-direction of the kinematic frame:

$$0.8 \leq (n_z)_K \leq 1.2, \tag{33}$$

which ensures a feasible solution regarding structural loads and passenger comfort. Additionally, all aircraft are prohibited from gaining altitude at this stage of the flight to limit the workload on the air traffic control officers (ATCO):

$$\gamma_K \leq 0. \tag{34}$$

4.2 Dynamic Constraints

Dynamic constraints are introduced to an optimal control problem to account for the dynamic behavior of a system, such as the aircraft. For a state space representation, they can take the form

$$\dot{\mathbf{x}} - \mathbf{f}(\mathbf{x}, \mathbf{u}) = 0. \tag{35}$$

In order to solve the optimal control problem numerically, the dynamic equations can be discretized by applying a collocation scheme. Here, a trapezoidal approximation of the state trajectory is employed, which is discussed in the next section.

Besides the aircraft model, an auxiliary state is introduced within this bi-level approach to obtain the sensitivity of required time separation due to the minimum distance violation with respect to the arrival time

$$\frac{\partial \Delta t_{ji,d}}{\partial \hat{t}_i}, \tag{36}$$

which is required in equation (16) that is in turn provided to the interior point solver of the upper level problem. The equation of motion for this auxiliary state switches from 0 to 1 at the point, when the following aircraft passes the point of minimum distances separation to the FAF. Consequently, the preceding aircraft must pass the point before the time point of the switch. Integrating the function over the remaining flight time of the following aircraft yields the time separation required to ensure the minimum distance separation $\Delta t_{ji,d}$. To mitigate numerical problems at the switch, the function is relaxed using a hyperbolic tangent function:

$$\dot{t}_{aux} = \frac{1}{2}\left(\tanh\left(k \cdot \left(d_{min} - d\left(\varphi, \lambda\right)\right)\right) + 1\right), \tag{37}$$

where the parameter k can be used to control the relaxation of the step.

4.3 Direct Collocation Method

Due to increasing computational power over the last decades, direct optimal control methods have become competitive to the indirect strategies developed by Pontryagin and Hestenes in the 1950's. Extensive literature on direct methods, e.g. in [12, 13, 14], and their application can be found, e.g. [2, 15, 16]. The trapezoidal collocation approach persued within this paper, i.e. the discretization of all state and control variables with respect to time and replacement of the dynamic constraints by a set of equality constraints (defects) belongs to this class of methods. Here, the time derivative of the state vector $\dot{\mathbf{x}}$ during a single time step

$$h_k = t_{k+1} - t_k \tag{38}$$

is approximated by the mean value of the state derivative at both endpoints, leading to a quadratic polynomial approximation of the trajectory. This integration step is subtracted from the result of the actual difference given by the discretized states across that time interval, leading to the defect equation

$$\mathbf{c}_{d,k} = \mathbf{x}_{k+1} - \mathbf{x}_k - \frac{h_k}{2}\left(\mathbf{f}\left(\mathbf{x}_k, \mathbf{u}_k\right) + \mathbf{f}\left(\mathbf{x}_{k+1}, \mathbf{u}_{k+1}\right)\right) = 0. \tag{39}$$

The discretization leads to a large nonlinear pro-

gram (NLP) with the respective Lagrange function

$$\begin{aligned} L(\mathbf{x},\mathbf{u},\sigma,\lambda,\mu) &= J(\mathbf{x}_1) + \sigma^T \psi(\mathbf{x}_0,\mathbf{x}_1) \\ &+ \sum_{k=0}^{N-1} \lambda_{k+1}^T c_{d,k} \\ &+ \sum_{k=0}^{N} \mu_k^T \mathbf{c}(t_k,\mathbf{x}_k,\mathbf{u}_k) \\ &+ \lambda_{\hat{t}} c_{\hat{t}}(\hat{t}), \end{aligned} \tag{40}$$

where ψ contains both the initial and final boundary conditions and $\mathbf{c}$ comprises all path constraints of the problem. Finally, the arrival time assignment constraint

$$c_{\hat{t}}(\hat{t}) \tag{41}$$

is a function of the parameter $\hat{t}$, i.e. the solution of the optimal control problem is also a function of this parameter.

The transcription of the optimal control problem into an NLP is performed by utilizing the optimal control tool *FALCON.m*[1] [17], which implements automated functionality to generate and evaluate the objective and constraint functions of the NLP. Additionally, a tool is included that automatically generates the respective Jacobian, which is provided to IPOPT [8] that is employed as the numerical solver for the lower level problems in this work.

4.4 Post optimal sensitivity analysis

For a given parameter $\hat{t}$, the Lagrange function is stationary at the optimal solution (KKT condition):

$$\nabla_{\mathbf{z}} L(\mathbf{z},\mathbf{p}) = 0, \tag{42}$$

where

$$\mathbf{z} = (\mathbf{x},\mathbf{u},\sigma,\lambda,\mu)^T \tag{43}$$

denotes the vector comprising all optimization variables and Lagrange multipliers and $\mathbf{p}$ the vector containing all parameters of the problem, i.e. $\hat{t}$ in this particular case.

Furthermore, in a small neighborhood of the parameters $\mathbf{p}$, the implicit function theorem can be applied [18, 19]:

$$\nabla^2_{\mathbf{zz}} L \cdot \frac{d\mathbf{z}}{d\mathbf{p}} + \nabla^2_{\mathbf{zp}} L = 0 \tag{44}$$

Rearranging the terms yields an equation for the post optimal sensitivities of the optimization variables and Lagrange multipliers with respect to the problem parameters:

$$\frac{d\mathbf{z}}{d\mathbf{p}} = -\left(\nabla^2_{\mathbf{zz}} L\right)^{-1} \nabla^2_{\mathbf{zp}} L, \tag{45}$$

[1] http:\\www.falcon-m.com

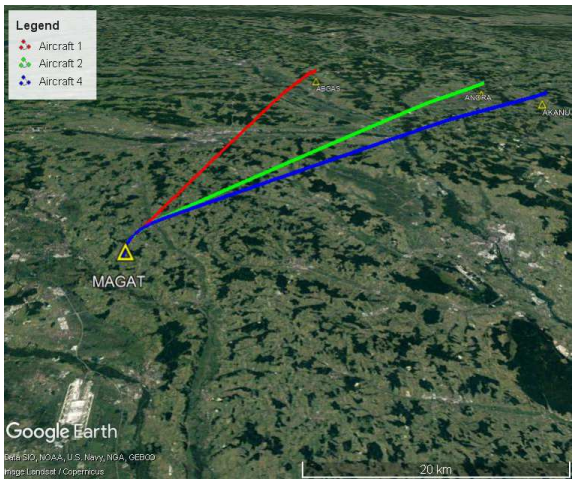

Figure 3: Google earth visualization of the trajectories of arriving aircraft.

which contain the sensitivity $\frac{\partial m_{1,1}}{\partial \hat{t}_1}$ required in equation (14). Finally, the second order sensitivity of the objective function with respect to the problem parameter can be obtained [19].

5 CASE STUDY

The algorithm is tested using a small case study comprising three arriving and one departing aircraft. The solution is found within 20 *min*, 58.7 *s* on a desktop computer equipped with a Core i7-4770 CPU @ 3.40GHz and 16 GB of RAM running Windows 10, which is significantly faster than the genetic algorithm employed in [5], however slower than the homotopy approach presented in [6].

The optimal trajectories under the constraint of fixed arrival times are shown in Fig. 3. All trajectories show a typical resemblance to the Dubin's path, which is the shortest path between two points of fixed heading under a constrained turn radius. This is an indication of the validity of the algorithm, as well as a sufficient time separation at the initial approach fix.

Furthermore, the departing aircraft is able to takeoff at the desired departure time of 20 *min*. It has to be noted that this is subject to the weighing factor θ, which can be used to adjust the priorities of an ontime departure and a reduction of fuel consumption.

6 CONCLUSIONS

In the paper, we introduced a bi-level algorithm to simultaneously solve the problems of sequencing arriving and departing aircraft, as well as finding optimal trajectories. The algorithm shows a strong performance compared to the solution of combinatorial

problems, which suffer from the curse of dimensionality. In contrast, the assignment of optimal arrival times allows for the application of gradient-based methods in the upper optimization level. However, a global optimum cannot be guaranteed for either algorithm, with the exception of some specific methods that require long computation times.

Further research in this field will include the search for strategies to find global optima by combining the advantages of several methods, e.g. by combining global algorithms with the presented method. Moreover, the properties of the continuous problem will be exploited by further analyzing the solution of the bi-level problem, including the calculation of post-optimal sensitivities with respect to uncertain parameters.

References

[1] SESAR Joint Undertaking. European atm master plan, 2012.

[2] Matthias Bittner, Matthias Rieck, Benedikt Grüter, and Florian Holzapfel. Optimal conflict free approach trajectories for multiple aircraft. In *ENRI Int. Workshop on ATM/CNS (EIWAC2015)*. Tokyo, Japan, 2015.

[3] Matthias Bittner, Matthias Rieck, Benedikt Grüter, and Florian Holzapfel. Optimal approach trajectories for multiple aircraft considering disturbances and configuration changes. In *ICAS 30th International Congress of the International Council of the Aeronautical Sciences*, 2016.

[4] Daichi Toratani, Seiya UENO, and Takehiro HIGUCHI. Simultaneous optimization method for trajectory and sequence for receding horizon guidance in terminal area. *SICE Journal of Control, Measurement, and System Integration*, 8(2):144–153, 2015.

[5] Benedikt Grüter, Matthias Bittner, Matthias Rieck, Johannes Diepolder, and Florian Holzapfel. Optimal sequencing in atm combining genetic algorithms and gradient based methods to a bilevel approach. In *ICAS 30th International Congress of the International Council of the Aeronautical Sciences*, 2016.

[6] Benedikt Grüter, Matthias Bittner, Matthias Rieck, Johannes Diepolder, and Florian Holzapfel. Bi-level homotopic aircraft sequencing using gradient-based arrival time assignment and direct optimal control. In *57th Israel Annual Conference on Aerospace Sciences*, 2017.

[7] International Civil Aviation Organization. Air traffic management: Doc 4444.

[8] Andreas Wächter and Lorenz T. Biegler. On the implementation of an interior-point filter line-search algorithm for large-scale nonlinear programming. *Mathematical programming*, 106(1):25–57, 2006.

[9] R. Fletcher. *Practical methods of optimization*. Wiley, Chichester and New York, 2nd ed. edition, 2010.

[10] Rudolf Brockhaus, Wolfgang Alles, and Robert Luckner. *Flugregelung*. Springer, Dordrecht, 2011.

[11] A. Nuic. User manual for the base of aircraft data (bada) revision 3.11. *Atmosphere*, 2010:001, 2010.

[12] J. Z. Ben-Asher. *Optimal Control Theory with Aerospace Applications*. AIAA education series. American Institute of Aeronautics and Astronautics, 2010.

[13] Christof Büskens. *Optimierungsmethoden und Sensitivitätsanalyse für optimale Steuerprozesse mit Steuer- und Zustands-Beschränkungen: Münster (Westfalen), Univ., Diss., 1998*. 1998.

[14] Matthias Gerdts. *Optimal control of ODEs and DAEs*. De Gruyter textbook. De Gruyter, Berlin and Boston, 2012.

[15] Florian Fisch, Matthias Bittner, and Florian Holzapfel. Optimal scheduling of fuel-minimal approach trajectories. *Journal of Aerospace Operations*, 2014.

[16] Maximilian Richter, Matthias Bittner, and Florian Holzapfel. Noise minimal approaches on parallel runways. In *4th International Air Transport and Operations Symposium*, 2013.

[17] Matthias Rieck, Matthias Bittner, Benedikt Grüter, and Johannes Diepolder. Falcon.m: User guide. 2016.

[18] Anthony V. Fiacco. *Introduction to sensitivity and stability analysis in nonlinear programming*, volume 165 of *Mathematics in science and engineering*. Acad. Press, New York, 1983.

[19] Christof Büskens and Helmut Maurer. Sqp-methods for solving optimal control problems with control and state constraints: adjoint variables, sensitivity analysis and real-time control. *Journal of Computational and Applied Mathematics*, 120(1–2):85–108, 2000.